ISAR IMAGE 3D RECONSTRUCTION BASED ON RADAR NETWORK

Le Kang [1,2], Ying Luo [1,2,3], Tian-chi Sun[1,2], Xiao-wen Liu[1,2], Jia Liang[1,2]

[1]Institute of Information and Navigation, Air Force Engineering University, Xi'an 710077, China
[2]Collaborative Innovation Center of Information Sensing and Understanding, Xi'an, 710077, China
[3] Key Laboratory for Information Science of Electromagnetic Waves (Ministry of Education), Fudan University, Shanghai, China.

***Abstract*—Traditional 2-D inverse synthetic aperture radar (ISAR) imaging can be regard as an inverse problem to reconstruct the target's scattering distribution from the echo. However, 2-D ISAR cannot represents the 3-D geometric relationship between the radar and targets, so it can only obtain the target's scattering projection on the corresponding Range-Doppler plane rather than the target's 3-D scattering distribution. To constitute a radar network, several radars should be selected from the all available radars. Because the distribution of the selected radars make an impact on the imaging performance, the distribution optimization should be considered in radar network imaging. In this paper, a novel 3-D ISAR image reconstruction method based on the optimized radar network is proposed. Firstly, the 3-D ISAR image reconstruction model is constructed by combining the projection relationship of each ISAR image and the distribution optimization. Secondly, the corresponding algorithm is proposed. With the proposed method, the optimal radar network distribution and the 3-D ISAR image can be obtained effectively. Finally, experiments demonstrate the performance of the proposed method.**

***Index Terms*—**radar network, image reconstruction, three-dimensional (3-D) inverse synthetic aperture radar (ISAR).

I. INTRODUCTION

Three-dimensional (3-D) inversed synthetic aperture radar (ISAR) image, compared with 2-D ISAR image, has attracted a wide attention, as it can provide more detailed information for target recognition. In recent years, 3-D ISAR imaging methods can be mainly summarized as three different frames [1] [2].

The first type is interferometric ISAR techniques, in which the 3-D spatial information is extracted from the interferometric phase difference between the multiple ISAR images. Due to the process of the phase difference between 2-D ISAR images, only one height value can be obtained for one pixel in the 2-D ISAR image, which means that the scatterers with same maps in imaging plane cannot be separated [3] [4].The second type, ISAR movie, is to utilize a sequence of ISAR images to provide 3-D reconstruction of a target. In this method, as the positions of the scatterers are determined by processing the tracks on the ISAR image plane, along observation time and the target track are strictly required [5]. The third kind,3-D ISAR imaging based on multiple-input multiple-output (MIMO) radar (including linear array), as a direct extension of the 2-D ISAR concept, can obtain the resolution in two cross-range directions through a 2-D synthetic aperture and the range resolution through wideband waveforms. To accomplish it, a complex physical system together with a dense three dimension sampling are required, which will cause large amount of data [6][7].

Compared with the aforementioned methods, the radar network utilizes multiple separated radar observations in different angles, which can reduce the complexity of the physical system and image the stealth target [8] [9]. However, there is little research on the relationship between the reconstruction performance and the distribution of radar network.

In this paper, the feasibility of 3-D ISAR image reconstruction by radar network has been verified. Combining the relationship between the 2-D ISAR image and the target's projection on the imaging plane, the 3-D ISAR image reconstruction model is constructed by minimizing the absolute error between the 2-D ISAR image and the projection of the spatial points. In this model, measurement matrix plays a crucial role to guarantee the reconstruction performance. To utilize the optimized distribution of radar network, the 3-D ISAR image reconstruction model can be solved by the proposed algorithm. Finally, the experiments demonstrate the reconstruction performance of the proposed method is better than that without distribution optimization of radar network.

This work was supported by the National Natural Science Foundation of China under Grant no. 61631019.

II. RADAR NETWORK 3-D IMAGING SYSTEM AND MODEL

A. Radar Network System geometry

For one radar in the radar network, as shown in Fig. 1, the target is projected onto the imaging plane. $(\mathrm{R},\mathrm{X},\mathrm{Y},\mathrm{Z})$ denotes a local Cartesian coordinate and the origin R is the location of the radar. The point P denote the target center point and the imaging reference point. The plane *abcd* denotes the imaging plane and the coordinate system is denoted by $(\mathrm{P},\mathrm{U},\mathrm{W})$, which is determined by the line of sight (LOS) $\overrightarrow{\mathbf{RP}}$ and the velocity vector $\mathbf{V}$.

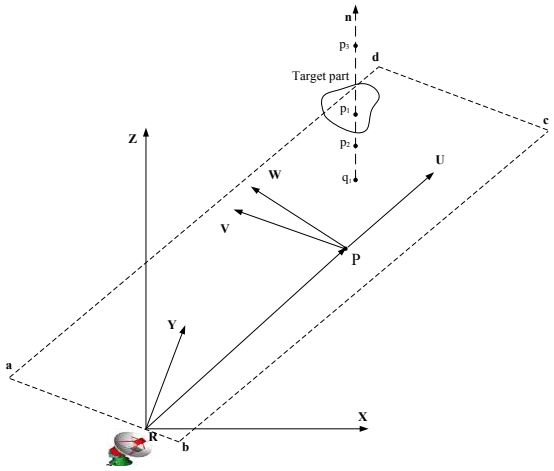

Fig. 1.Geometry model for the projection of the spatial point.

The point q_1 is one of the points on the 2-D ISAR image of the target. The point p_1, p_2 and p_3 are three spatial points and their projection coincide on the imaging plane. There is only one scatterer in p_1 but no scatterer in p_2 and p_3. Therefore, it is essential to ensure the feasible spatial points whose projection coincide on the 2-D ISAR image of the target, and then confirming which positions contain the scatterers of the target. Therefore, based on the radar network, the 3-D ISAR image will be constructed by estimating the position of the scatterers.

B. 3-D ISAR image reconstruction model

Translate the coordinate $(\mathrm{R},\mathrm{X},\mathrm{Y},\mathrm{Z})$ to $(\mathrm{P},\mathrm{X},\mathrm{Y},\mathrm{Z})$ where the origin P is the imaging reference point. For any point A on the target, B is the projection point on the plane *abcd* and the $\overrightarrow{\mathbf{PB}}=c_1\boldsymbol{u}+c_2\boldsymbol{w}$, where $\boldsymbol{u}$ and $\boldsymbol{w}$ are the normal vector of $\overrightarrow{\mathbf{PU}}$ and $\overrightarrow{\mathbf{PW}}$ and $\mathbf{n}$ is the normal vector perpendicular of the imaging plane. The projection relationship can be expressed as

$$\begin{cases}\left(\overrightarrow{\mathbf{PA}}-\overrightarrow{\mathbf{PB}}\right)^T\boldsymbol{u}=\vec{\mathbf{0}}\\ \left(\overrightarrow{\mathbf{PA}}-\overrightarrow{\mathbf{PB}}\right)^T\boldsymbol{w}=\vec{\mathbf{0}}\end{cases}\Leftrightarrow \boldsymbol{D}^T\left(\overrightarrow{\mathbf{PA}}-\boldsymbol{D}\begin{bmatrix}c_1\\c_2\end{bmatrix}\right),\quad \boldsymbol{D}=[\boldsymbol{u},\boldsymbol{w}] \tag{1}$$

Then the projection point B is located at (c_1,c_2) in $(\mathrm{P},\mathrm{U},\mathrm{W})$ and the position can be obtained by

$$\begin{bmatrix}c_1\\c_2\end{bmatrix}=\left(\boldsymbol{D}^T\boldsymbol{D}\right)^{-1}\boldsymbol{D}^T\overrightarrow{\mathbf{PA}}=\boldsymbol{\Phi}\overrightarrow{\mathbf{PA}} \tag{2}$$

where $\boldsymbol{\Phi}$ is the projection matrix.

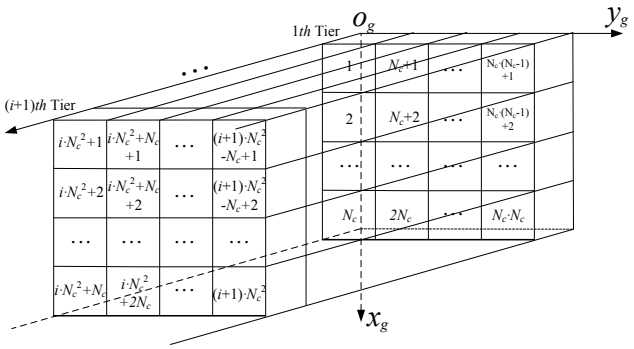

Fig. 2.Numbering for the cells of the grid model. The 1*th* and (*i*+1)*th* tier of the grid model are numbered as shown above.

As shown in Fig. 2, the 3-D grids are used to discretize the target space, all of the scatterers are assumed to be located at the cube and the target center point P is in the center cell. Then all of the scatterers can be projected on the imaging plan as

$$\mathrm{F}(\boldsymbol{X})=\boldsymbol{\Phi}\,\mathrm{Vec}(\boldsymbol{X}),\ \mathrm{Vec}(\boldsymbol{X})=\left[\overrightarrow{\mathbf{PT}_1},\overrightarrow{\mathbf{PT}_2},\ldots,\overrightarrow{\mathbf{PT}_{N_c^3}}\right] \tag{3}$$

where $\mathrm{F}(\cdot)$ denotes the projection operation, $\mathrm{Vec}(\cdot)$ denotes the vectorization operation to line up the coordinate of the spatial points and the matrix $\boldsymbol{X}$ denotes the 3-D grid model contains only 0 and 1, $\boldsymbol{\Phi}$ is the projection matrix. The element 1 and 0 in the matrix $\boldsymbol{X}$ respectively represent whether the cell contains the spatial points or not.

If the projections of the 3-D target on the imaging planes have the minimal square sum of minus value with the ISAR images, the 3-D target is considered to have a good reconstruction performance. Therefore, the least amount of the spatial points is added into the cost function. According to the difference between the ISAR images and the corresponding projections, the radar network 3-D ISAR image reconstruction model can be expressed by

$$\begin{aligned}&\textit{minimize}\quad \omega\cdot\sum_{z=1}^{N_c}\sum_{y=1}^{N_c}\sum_{x=1}^{N_c}\boldsymbol{X}(x,y,z)+\sum_{m=1}^{M}\left\|\mathrm{F}_m(\boldsymbol{X})-\boldsymbol{I}_m\right\|_2\\ &s.t.\quad\begin{cases}\boldsymbol{X}(x,y,z)\in\{0,1\}\\ \boldsymbol{X}\subseteq\boldsymbol{G}\end{cases}\end{aligned} \tag{4}$$

where the $\boldsymbol{G}$ is a matrix set representing the search space

of all possibility of the 3-D distribution, ω denotes the weighting parameter of the sparsity, M denotes the number of the radar in the radar network, $\mathbf{F}_m(\cdot)$ denotes the projection operation for the m-th radar, $\boldsymbol{I}_m$ is the 2-D ISAR image obtained by the m-th radar. Therefore, the 3-D ISAR image will be reconstructed by solving the aforementioned model.

C. Distribution Optimization of Radar Network

Due to the target could move toward the radar along the line-of-sight direction and to simplify the reconstruction model, the radar network is constituted by three radars in this paper. Then the error item in the objective function can be detailed as

$$\begin{aligned}&\sum_{m=1}^{3}\left\|\mathrm{F}_m(\boldsymbol{X})-\boldsymbol{I}_m\right\|_2\\&=\sum_{m=1}^{3}\left(\boldsymbol{\Phi}_m\,\mathrm{Vec}(\boldsymbol{X})-\boldsymbol{I}_m\right)^T\left(\boldsymbol{\Phi}_m\,\mathrm{Vec}(\boldsymbol{X})-\boldsymbol{I}_m\right)\\&=\left\|\boldsymbol{S}\,\mathrm{Vec}(\boldsymbol{X})^T-\boldsymbol{\Gamma}\right\|_2\end{aligned}\tag{5}$$

where $$\boldsymbol{S}=\left[\boldsymbol{\Phi}_1,\boldsymbol{\Phi}_2,\boldsymbol{\Phi}_3\right],\boldsymbol{\Gamma}=\left[\boldsymbol{I}_1,\boldsymbol{I}_2,\boldsymbol{I}_3\right]\tag{6}$$

and (4) can be regarded as a compressed sensing (CS) model [10], in which the measurement matrix makes critical effect on the reconstruction performance. From the different criteria of measurement matrix, the worst-case mutual coherence is chosen because of the low computational cost. The worst-case mutual coherence of $\boldsymbol{S}$ is defined as [11]:

$$\mu(\boldsymbol{S},\boldsymbol{S})=\max_{i,k,i\neq k}\mu(s_i,s_k)=\max_{i,k,i\neq k}\frac{\langle s_i,s_k\rangle}{\|s_i\|_2\|s_k\|_2}\tag{7}$$

where s_i is the i-th column of $\boldsymbol{S}$ and $\langle\cdot\rangle$ denotes the inner product operation. From (6), we define the matrix $\boldsymbol{U}(\boldsymbol{S})$ with the element $\mu(s_i,s_k)$ and it can be further expressed as

$$\boldsymbol{U}(\boldsymbol{S})=\begin{bmatrix}\boldsymbol{U}(\boldsymbol{\Phi}_1)&\boldsymbol{U}(\boldsymbol{\Phi}_1,\boldsymbol{\Phi}_2)&\boldsymbol{U}(\boldsymbol{\Phi}_1,\boldsymbol{\Phi}_3)\\\boldsymbol{U}(\boldsymbol{\Phi}_2,\boldsymbol{\Phi}_1)&\boldsymbol{U}(\boldsymbol{\Phi}_2)&\boldsymbol{U}(\boldsymbol{\Phi}_2,\boldsymbol{\Phi}_3)\\\boldsymbol{U}(\boldsymbol{\Phi}_3,\boldsymbol{\Phi}_1)&\boldsymbol{U}(\boldsymbol{\Phi}_3,\boldsymbol{\Phi}_2)&\boldsymbol{U}(\boldsymbol{\Phi}_3)\end{bmatrix}\tag{8}$$

According to the definition in (7), the worst-case mutual coherence of $\boldsymbol{S}$ can be rewritten as

$$\mu(\boldsymbol{S},\boldsymbol{S})=\max\begin{Bmatrix}\mu(\boldsymbol{\Phi}_1,\boldsymbol{\Phi}_1),\mu(\boldsymbol{\Phi}_1,\boldsymbol{\Phi}_2),\\\mu(\boldsymbol{\Phi}_1,\boldsymbol{\Phi}_3),\mu(\boldsymbol{\Phi}_2,\boldsymbol{\Phi}_2),\\\mu(\boldsymbol{\Phi}_2,\boldsymbol{\Phi}_3),\mu(\boldsymbol{\Phi}_3,\boldsymbol{\Phi}_3)\end{Bmatrix}\tag{9}$$

which means that the reconstruction performance can be judged by a new evaluation index, the maximum worst-case mutual coherence between the projection matrixes of the whole radars. In the CS framework, small worst-case mutual coherence can produce high probability for good reconstruction performance. So, assume the position of radars is denoted by $\boldsymbol{R}$ and the radar network optimization can be expressed as

$$\underset{\boldsymbol{R}_k}{minimize}\left\{\max_{1\le i,j\le 3}\mu(\boldsymbol{\Phi}_i,\boldsymbol{\Phi}_j)\right\}\quad s.t.\quad \boldsymbol{R}_k\in\mathbb{R}^3,1\le k\le 3\tag{10}$$

which can be solved by Lloyd algorithm [12]. However, in the practical application, the position of radars are fixed and the number of the available radars is limited, which means that the $\boldsymbol{R}$ can only be chosen in a small fixed discrete set. For the small-sized problem, the exhaustion method is more effective.

III. 3-D ISAR IMAGE RECONSTRUCTION

The concrete steps of the radar network 3-D ISAR image reconstruction as follows: Step 1) Acquire the target parameters, including the velocity and the position, by the target tracking method. Step 2) Acquire the position of the available radars and obtain the optimized distribution of radar network. Step 3) Perform the Range-Doppler algorithm to obtain the ISAR image of every radar in the radar network. Step 4) Solve the 3-D ISAR image reconstruction model to acquire the scatterers distribution of the target.

As the elements of matrix $\mathbf{X}$ is only equivalent to 0 or 1, the optimization problem in (4) is 0-1 Programming. The genetic algorithm is an appropriate method to solve the 0-1 Programming. However, the matrix size of $\mathbf{X}$ is so large that the operation complexity of the genetic algorithm to solve the reconstruction model is too high. Therefore, it necessary to propose an algorithm to reduce the operation complexity in solving the 3-D ISAR image reconstruction model.

For different radars in the radar network, there is one set of feasible spatial points. It can be sought out by calculating the difference image with respect to every cell of the space grid model. The cell is considered as the feasible spatial point only when the square sum of the value of corresponding difference image is smaller than that of ISAR image. Therefore, the search scope is confirmed by calculating the intersection of every set of feasible spatial points and the new search scope is used in the genetic algorithm. Let the optimum matrix be denoted by $\mathbf{X}_{\text{opt}}$ .The proposed algorithm for solving the 3-D ISAR image reconstruction model is depicted in Table I.

TABLE I THE 3-D ISAR IMAGE RECONSTRUCTION ALGORITHM

Step 1) Input the target and the radar parameters.
Step 2)Distribution Optimization of Radar Network: Calculate the worst-case mutual coherence for the whole combinations of the radar network according to (9), and choose the radar network corresponding to the minimum value.
Step 3)Perform the Range-Doppler algorithm to obtain the ISAR image $\boldsymbol{I}_m$ of the m-*th* radar.
Step 4)

1. Define the 3-Dmatrix $\boldsymbol{C}$ as the 3-D grid model; Define $\boldsymbol{\gamma}=\{1,2,3,...,N_c^3-1,N_c^3\}$ as the index set of cells;
2. **For** $m=1:M$
   Set $\boldsymbol{C}=\mathbf{0}$, the set of feasible spatial points $\boldsymbol{\alpha}_m=\varnothing$;
   For $i=1:N_c^3$, where i is the index shown in Fig. 3.
   Set $\mathbf{C}(i)=1$;Calculate the $\mathbf{F}_m\left(\mathbf{C}(i)\right)$ according to (3) and $\left\|\mathbf{F}_m\left(\mathbf{C}(i)\right)-\mathbf{I}_m\right\|_2$;
   If $\left\|\mathbf{F}_m\left(\mathbf{C}(i)\right)-\mathbf{I}_m\right\|_2<\left\|\mathbf{I}_m\right\|_2$, do $\boldsymbol{\alpha}_m=\boldsymbol{\alpha}_m\cup i$;
   end
end
3. Update the search scope as $\boldsymbol{\beta}=\bigcap_{m=1}^{M}\boldsymbol{\alpha}_m$ and
$\mathbf{G}'=\{\mathbf{C}\,|\,\mathbf{C}(\boldsymbol{\gamma}-\boldsymbol{\beta})=\mathbf{0},\mathbf{C}\in\mathbf{G}\}$;
4. Solve the optimization problem in (4) by the genetic algorithm to obtain $\mathbf{x}_{\text{opt}}$;

To evaluate the imaging quality of the proposed method, the average estimation error of scatterer distance that could affect the 3-D image reconstruction results can be determined by.

$$\Lambda=E\left[\varepsilon_d(k,s)\right]=\frac{1}{S}\frac{1}{K}\sum_{s=1}^{S}\sum_{k=1}^{K}\varepsilon_d(k,s) \tag{11}$$

where $E[\cdot]$ denotes the expectation operator about all the K scatterers of S Monte Carlo runs. For each simulation, 50 Monte Carlo runs are carried out to calculate the scatterer distance estimation error Λ.

IV. Experiments

In this section, the simulation experiments are used to confirm the validity of the proposed method. As shown in Fig. 3(a), the target model is form as the set of 34 ideal scatterers and the scattering coefficients are assumed as unit. Let the side length of cube is 0.25 m. The required target parameters are shown in Table II.

TABLE II Parameters of the Target

	Velocity $\mathbf{V}$ (m/s)	Coordinates (x_0,y_0,z_0) (km)	Target length L_t (m)
Target	(-450.35,-50.5,0)	(11,10,0.75)	10

As shown in Fig. 3(b), the distribution of available radars is given by generating 20 random coordinates and the radar network is made up of three selected imaging radars. The selection criteria is accordance with the discussion from (5) to (10). The radar are assumed to transmit the linear frequency modulated signal with the carrier frequency $f_c=10\text{GZ}$, the pulse repetition frequency $\text{PRF}=1000\text{HZ}$ and the pulse duration $T_r=1\,\mu\text{s}$.

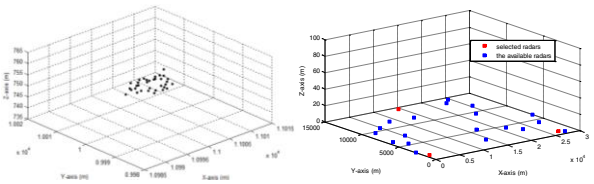

(a) (b)

Fig. 3. (a) The aircraft target model consisting of 34 ideal scatterers. (b) The distribution of available radars and the selected radar network

The ISAR imaging results of Radar 1 to 3obtained by the Range-Doppler algorithm and the corresponding projection images obtained by projection operation are shown in Fig. 4. The 3-D reconstruction results of target are shown in Fig. 5(a).In addition, the three-view of the target are presented in Fig. 5(b)-(d),where the black dots denote the position of target scatterers, the blue circles denote the reconstructed result obtained by the radar network with a random distribution and the red circles denote the reconstructed result obtained by the proposed method. As it can be seen, the red circles match better with the position of target scatterers than the blue circles. Furthermore, the estimation error Λ of the proposed method is calculated as 0.151, which is so small that can be accepted.

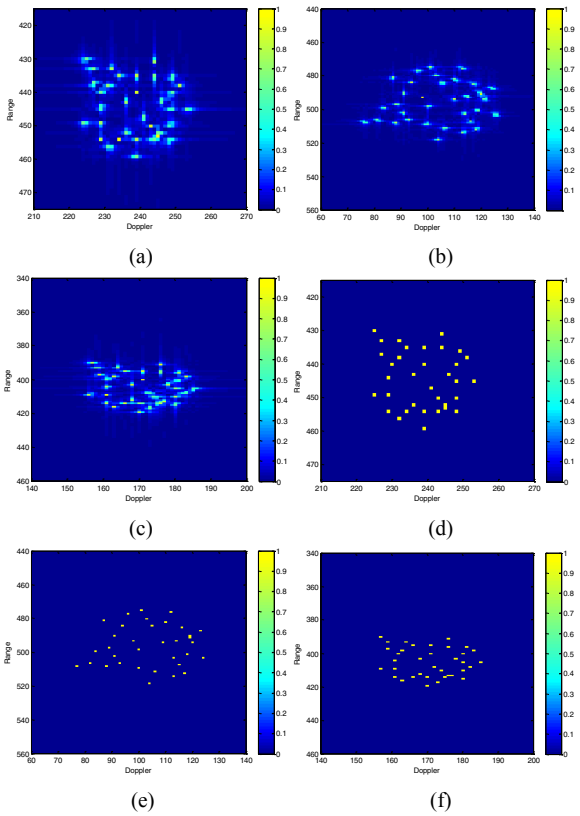

(a) (b)

(c) (d)

(e) (f)

Fig. 4. The ISAR imaging results and the projection images. (a) The imaging results of Radar 1. (b) The imaging results of Radar 2. (c) The imaging results by the Radar 3. (d) The projection image of Radar 1. (e) The projection image of Radar 2. (f) The projection image of Radar 3.

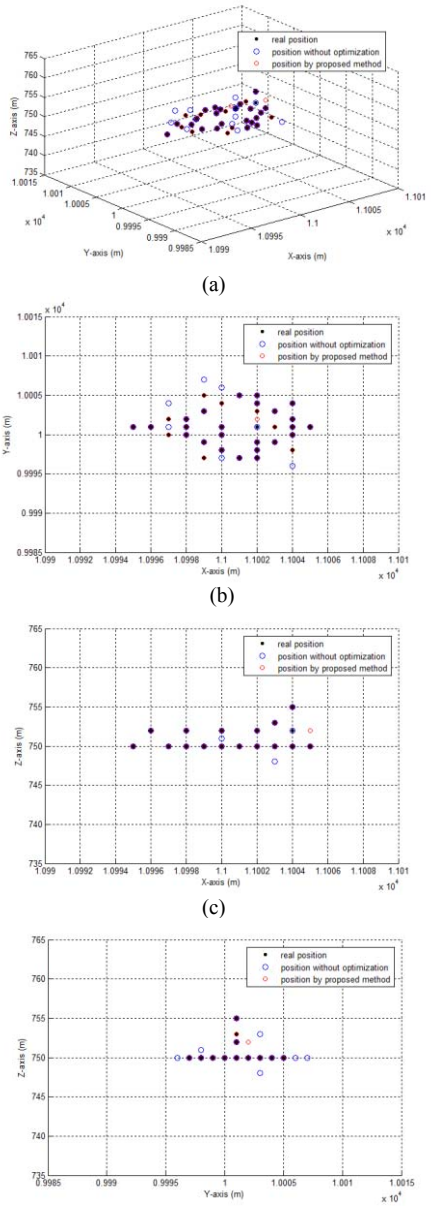

Fig. 5.The 3-D ISAR reconstruction result and the three-view

In fact, two main reasons may cause the ISAR 3-D reconstructed error. On the one hand, the position of the scatterer is assumed at the center of the corresponding grid cell. However, the hypothesis not exactly accurate because the position is continuous but the grid is discrete, which cause the modeling errors. On the other hand, the lower imaging resolution and the projection operation may also produce the error. Therefore, to improve the reconstruction precision, the one suggestion is to considering about the mismatch problem and another suggestion is to improve the resolution of the ISAR image.

V. CONCLUSIONS

In this paper, the radar network is formed by three imaging radars observing a target simultaneously. Firstly, the processing for projecting the spatial point onto the range-Doppler plane is analysised. In addition, to make us of the criteria of worst-case mutual coherence, combining with the property of projection matrix, the distribution optimization model of radar network is constructed. Moreover, by minimizing the reconstruction error, the3-D ISAR image reconstruction algorithm is proposed. Finally, the simulations of3-D ISAR image reconstruction are given and the reasons of the reconstructed error are discussed. The experimental results demonstrate that the3-D ISAR image based on the radar network can be obtained by the proposed method.

VI. REFERENCES

[1] X. Wang, B. F. Guo, and C. X. Shang,"3-D Reconstruction of Target Geometry Based on 2-D Data of Inverse Synthetic Aperture Radar Images," *J. of Electron. Inf. Technol.*, vol. 35, no. 10, pp. 2475-2480, Nov. 2013.

[2] X.Y. He, X. Y. Zhou, and T. J. Cui,"Fast3-D-ISAR Image Simulation of Targets at Arbitrary Aspect Angles Through Nonuniform Fast Fourier Transform (NUFFT),"*IEEE Trans. Antennas Propag.*, vol. 60, no. 5, pp. 2597-2602, May. 2012.

[3] M. Nasirian and M.H. Bastani, "A Novel Model for Three-Dimensional Imaging Using Interferometric ISAR in Any Curved Target Flight Path," *IEEE Trans. Geosci. Remote Sens.*, vol. 52, no. 6, pp. 3236-3245, Jun. 2014.

[4] Y. Wang and X. Li, "Three-Dimensional Interferometric ISAR Imaging for the Ship Target under the Bi-Static Configuration," *IEEE J. Sel. Topics Appl. Earth Observations Remote Sens.*, vol. 9, no. 4, pp. 1505-1520, Apr. 2016.

[5] K. Suwa, T. Wakayama, and M. Iwamoto, "Three-Dimensional Target Geometry and Target Motion Estimation Method Using Multistatic ISAR Movies and Its Performance," *IEEE Trans. Geosci. Remote Sens.*, vol. 49, no. 6, pp. 2361-2373, Jun. 2011.

[6] X. W. Hu, N.N. Tong, Y. S. Zhang, and Y. C. Wang, "3-D imaging using narrowband MIMO radar and ISAR technique," *Wireless Communications & Signal Processing*(WCSP) 2015, pp. 1-5. 15-17 Oct. 2015.

[7] W. Qiu, M. Martorella, J.X. Zhou, H. Z. Zhao, and Q. Fu, "Three-dimensional inverse synthetic aperture radar imaging based on compressive sensing," *IET Radar Sonar Navig.*, vol. 9, no. 4, pp. 411–420, Apr. 2015.

[8] Y.X. Bi, S. M. Wei, and J. Wang, "3-D reconstruction of high-speed moving targets based on HRR measurements," *IET Radar Sonar Navig*.2017, 11, vol. 11, no. 5, pp. 778–787, May. 2017.

[9] X. W. Liu, Q. Zhang, L, Jiang, J. Liang and Y. J. Chen, "Reconstruction of Three-Dimensional Images Based on Estimation of Spinning Target Parameters in Radar Network," *Remote Sensing*. 2018., vol. 10, no. 12, pp. 1997.

[10] E. J. Candes and M. B. Wakin, "An Introduction To Compressive Sampling," *IEEE Signal Process. Mag*. 2008, 25,21–30.

[11] P. Xia, S. Zhou and G. B. Giannakis, "Achieving the Welch bound with difference sets," *IEEE Trans. Inf. Theory*. 2005, 51, 1900–1907.

[12] P. Xia and G. B. Giannakis, "Design and analysis of transmit-beamforming based on limited-rate feedback," *IEEE Trans. Signal Process.* 2006, 54, 1853–1863.